Electrical properties of n-Zn$_{0.94}$Cd$_{0.06}$O/p-SiC heterostructures

I Shtepliuk, Volodymyr Khranovskyy, G Lashkarev, V Khomyak, V Lazorenko, A Ievtushenko, Mikael Syväjärvi, Valdas Jokubavicius and Rosita Yakimova

Linköping University Post Print

Tweet

N.B.: When citing this work, cite the original article.

Electrical properties of n-Zn$_{0.94}$Cd$_{0.06}$O/p-SiC heterostructures

I. Shtepliuk[1], V. Khranovskyy[2], G. Lashkarev[1], V. Khomyak[3], V. Lazorenko[1],

A. Ievtushenko[1], M. Syväjärvi[2], V. Jokubavicius[2] and R. Yakimova[2]

[1] *I. Frantsevich Institute for Problems of Material Science, NASU, 03680, Kiev, Ukraine*

[2]*Department of Physics, Chemistry and Biology (IFM), Linköping University, 58183 Linköping,*

Sweden

[3]*Chernivtsi National University, 58012, Chernivtsi, Ukraine*

Abstract

We report the low-temperature (250°C) fabrication of *n*-ZnCdO/*p*-SiC heterostructures by direct current magnetron sputtering (DC MS) technique. As-grown heterostructures exhibit diode characteristics: current–voltage measurements showed a typical rectifying characteristic of a p-n junction and the presence of series resistance. It is found that the turn-on voltage of heterostructures depends on the acceptor concentration in p-SiC. Via Cd doping of ZnO the energy barrier for holes can be lowered, which promotes the hole injection from the *p*-type layer to the *n*-type layer as well as favors the radiative recombination in the *n*-ZnCdO layer.

Keywords: ternary alloy, compositional fluctuation, photoluminescence, heterojunction

Introduction

Zinc Oxide is a promising semiconductor as a light emitting material for LEDs and LDs fabrication. However, p-type ZnO is still difficult to obtain. Alternatively, n-type ZnO may be grown on p-type semiconductors. To use the diversity and advantages of the optical transitions of ZnO [1] for the improvement of the electrical performance of n-ZnO/p-SiC heterostructures, it is necessary that the radiative recombination occurs in the n-type semiconductor. The advantage of SiC substrate is that

it has the same wurtzite crystal structure as ZnO, provides rather small lattice mismatch (of ~5% [2]) and has a close band-gap energy value [3]. Nevertheless, existing reports devoted to p-n-junction based on ZnO/SiC suggest that the radiative recombination mainly originates from defect-related states in the p-SiC layer [4, 5]. It is due to a prevailing electron injection from n-ZnO over the weak holes injection from p-SiC [3]. In order to overcome this problem, the energy barrier for holes should be lowered, whereas the energy barrier for electrons should be increased. Therefore, it is important to choose the heterostructure pair which would possess the small value of the valence band offset (VBO) exceeding the magnitude of the conduction band offset (CBO). Fang et al. found that using the $Zn_{0.95}Cd_{0.05}O$ layer in an n-ZnCdO/p-GaN structure allows reducing the energy barrier for holes to a value of -0.3 eV [6]. It means that the energy relationship is in favor of holes transferring from GaN to ZnCdO. Based on this observation we suggest that a similar effect may be also realized for an n-ZnCdO/p-SiC heterostructure. There is an extraordinary interest in ZnCdO ternary alloy caused by (i) the possibility to change its band-gap energy in the wide range depending on the cadmium content [7, 8], substrate type [9] and growth conditions [10-11]; (ii) the existence of visible luminescence covering the blue-green optical region; and (iii) the high optical transparency [12]. Many interesting phenomena like electroluminescence from n-ZnCdO/p-GaN heterojunction [6, 13, 14], green electroluminescence from ZnCdO multiple quantum-well light-emitting diodes [15] and luminescence enhancement effects of deuterium in ZnO/ZnCdO quantum wells [12] have already been reported. Nevertheless, the growth of $Zn_{1-x}Cd_xO$ alloys is complicated by the solid phase miscibility gap [16], which gives rise to a compositional inhomogeneity, and thus, local variations in the fundamental energy gap. Direct evidence for a phase separation in $Zn_{1-x}Cd_xO$ layers with $0.03<x<0.2$ has been obtained from the low temperature cathodoluminescence microscopy [17]. The phenomenon of phase separation in ZnCdO was also investigated by means of a combination of structural/optical measurements [18]. It was revealed the presence of a new, not usually considered, zinc-blende-ZnCdO phase in addition to commonly discussed wurtzite and rock-salt phases [18]. Above-mentioned factors complicate the understanding of the recombination

radiative processes in p–n heterojunctions based on ZnCdO. In this regard, the choice of the appropriate growth interface (i.e. kind of substrate) may become crucial factor for control of the compositional fluctuations/structure quality/Cd solubility, minimization of the stress/strain at the heterointerface, which can introduce the "composition pulling effect", and the improvement of the electrical properties of the p–n heterojunctions.

In this paper, we report on the structural, optical and electrical properties of as-grown n-ZnCdO/p-SiC heterojunctions. The originality of the present paper is that it reveals the effect of the acceptor concentration in p-SiC on the electrical properties of ZnCdO-based heterostructures, which has not been studied before. Additionally, possible mechanisms of the alloy composition influence on the luminescence are proposed and discussed. It is shown that it is necessary to have higher hole concentration ($>10^{18}$cm^{-3}) in the p-type SiC to turn on the intensive hole injection into the active region.

Experimental details

The ZnCdO films were fabricated on p-type boron doped SiC epilayers. The p-type SiC films were grown by the sublimation epitaxial method on n-SiC commercial substrate. We have used two SiC epilayers with different acceptor concentrations. Thus, the acceptor concentrations (boron) in the p-SiC thin films were around 1×10^{18} cm^{-3} (substrate was marked as "p") and 1×10^{19} cm^{-3} ("p$^+$"). The different concentrations aimed to explore possible influence on the electrical performance of the designed heterojunction. The thickness of the epilayers was about 325 and 150 μm for p and p+SiC, respectively. The ZnCdO ternary alloys were deposited by the direct current (dc) magnetron sputtering technique at the substrate temperature of 250°C. A disc of 90%zinc–10%cadmium alloy of 100 mm diameter with a purity of 99.99% was used as a target. High purity argon and oxygen were used as the sputtering and the reactive gases, respectively. The target-to-substrate distance was 40 mm. The chamber was pumped to a base pressure of 10^{-4} Pa before deposition. The films were grown in the ambient with the Ar/O$_2$ ratio of 4:1. The dc power was maintained at 100 W. A shadow mask was used to cover a selected part of the p-SiC substrate for further deposition of the

ohmic contacts on the p-SiC. The thickness of the films was ~1.5 μm for all samples, determined from the SEM images of the cross section of the films. Thin layers of Ni/Cr/Al and Ti/Al were applied as ohmic contacts. Aluminum contacts of a diameter 0.5mm were evaporated onto the SiC surfaces. The fabricated contacts on SiC films show linear $I-V$ characteristics, i.e. Ni/Cr/Al and Ti/Al metal multi-layers form the ohmic contacts to SiC films. The configuration of the device is illustrated schematically in Figure 1. The electrical properties of the device structure were evaluated using two-point probe current-voltage (I–V) characteristics [19]. The $I-V$ measurements were performed with top-to-back contacts; specifically, Al metal were deposited on the top ZnCdO surface without an annealing process, and Ni/Cr/Al (Ti/Al) metals on the backside of the SiC substrate, as schematically shown in Fig. 1. The microstructure and morphology of the films were studied by scanning electron microscopy (SEM) using a Leo 1550 Gemini SEM operated at voltages ranging from 10 to 20 kV and using a standard aperture value of 30 μm. The crystal structure of the samples was investigated by XRD method, where a Cu $K\alpha_1$ (λ = 0,154056 nm) source was used. The light emission was investigated by micro-photoluminescence carried out at room temperature with a frequency doubled Nd:YVO laser as continuous wave excitation source, giving a wavelength λ=266 nm. The emitted luminescence was collected and mirrored into a single grating 0.45 m monochromator equipped with a liquid nitrogen cooled Si-CCD camera with a spectral resolution of about 0.1 meV. The excited area was around 10 μm^2 providing an excitation density of 2 - 400 W/cm^2.

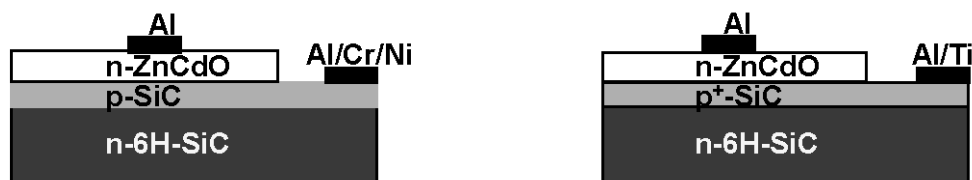*Fig. 1. Schematic illustration of n-ZnCdO/p-6H-SiC heterostructure devices*

Results and discussion

The grown ZnCdO films in general demonstrate a microstructure that is typical for sputtered films. The structure experiences a dense coverage of grains that are not obviously hexagonally faceted. This structure is due to the high deposition rate and a low growth temperature (Fig. 2 a, b). The average grain size estimated from SEM analysis was 200 nm ± 50 nm. Also a rather rough surface was observed. Some evidences of the substrate off cut can be observed: slightly tilted grains are the result of partial step flow growth, induced by the steps on the p-type epilayer.
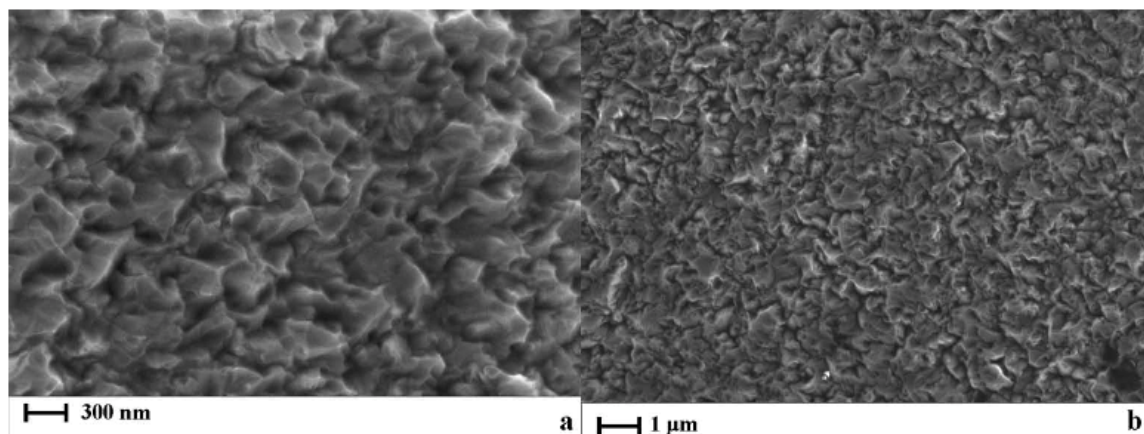

Fig.2 SEM images of ZnCdO films grown on the p (a) and p$^+$ (b)- SiC epitaxial layer. Scale bars are different on different images.

The typical XRD pattern (Fig. 3) of the heterojunctions indicates that the ZnCdO films were highly textured along the *c* axis. The XRD data of both studied films accurately correspond to that of JCPDS card No.36-1451 for hexagonal wurtzite structure of ZnO. This suggests that the introduction of cadmium atoms does not change the ZnO crystal structure [8, 14]. The observed (002) peak of ZnCdO was found to be shifted towards a lower 2θ angle (by 0.23°) than that of pure bulk ZnO (see Fig. 3). It is associated with the fact that the replacement of smaller Zn ions by larger Cd ions results in expansion of the ZnO lattice. It should be noted that we have dealt with two simultaneous competitive influencing the (002) peak position: (i) lattice mismatch (LM) and (ii) Cd incorporation. LM effect should lead to a displacement of the (002) peak towards higher Bragg's angle (due to compressive stresses), whereas the cadmium incorporation should cause lattice

expansion, appearance of the tensile stresses and shift of the main diffraction peak to smaller angle, respectively.
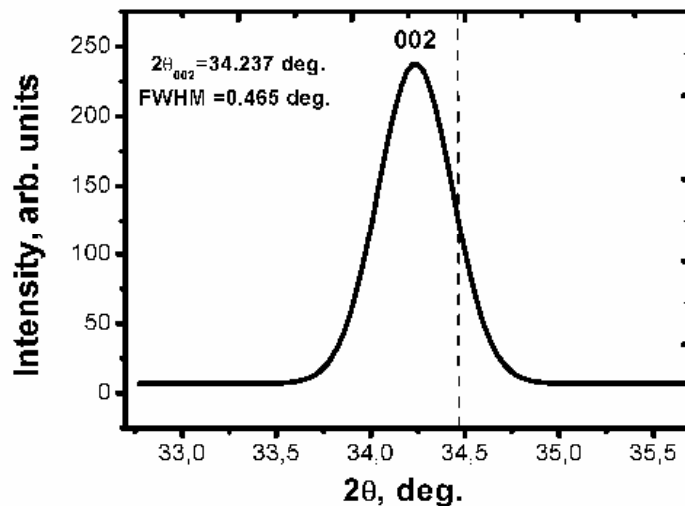

Fig.3. A typical XRD pattern of the n- ZnCdO film grown on the p-SiC substrate. Vertical line is

corresponded to (002) peak position for strain-free undoped ZnO [20]

Taking into account the similarity of the crystal structures as well as small lattice and thermal mismatch (TM) between ZnO and SiC, we have concluded that Cd incorporation effect is prevailing but is partially compensated by the lattice mismatch. We have neglected the TM effect on the (002) peak position, because the growth in our case is at rather low temperature. No additional diffraction peaks related to second phases (cubic CdO or metallic Cd) are observed. We have performed EDX analysis in order to study the Cd spatial distribution or to reveal its segregation in the film. The average Cd content was found to be~6 at.%.

We studied the electrical properties of the n-ZnCdO/p-SiC heterostructures. Figure 4 shows an equilibrium energy band diagram of the p-n heterojunction between p-SiC and n-ZnCdO, which was constructed in terms of the Anderson model [21]. According to the two semiconductors that are in contact, the energy barrier ΔE_C for electrons is $\Delta E_C = \chi_{ZnCdO} - \chi_{SiC} = 4.4 - 3.3 = 1.1$ eV, whereas the energy barrier ΔE_V for holes is: $\Delta E_V = E_{gZnCdO} + \Delta E_C - E_{gSiC} = 2.87 + 1.1 - 3.03 = 0.94$ eV. It should be noted that in the case of ZnCdO, the electron affinity is assumed to be between 4.3eV (ZnO) and

4.5eV (CdO) [22]. Therefore, we have used the average value of 4.4 eV. Here the band-gap (E_g) of ZnCdO is 2.87 eV and that of 6H-SiC is 3.03 eV. ΔE_V has a smaller value than ΔE_C, which means that the electron injection from n-ZnO to p-SiC is smaller than the hole injection from p-SiC to n-ZnCdO. In other words, under forward bias, the energy relationship is in favor of holes transferring from p-SiC to ZnCdO. Thus, we conclude that the Cd incorporation into ZnO matrix can lower the value of the valence band offset from 1.61 eV for pure ZnO [23] to 0.94 eV for $Zn_{0.94}Cd_{0.06}O$.
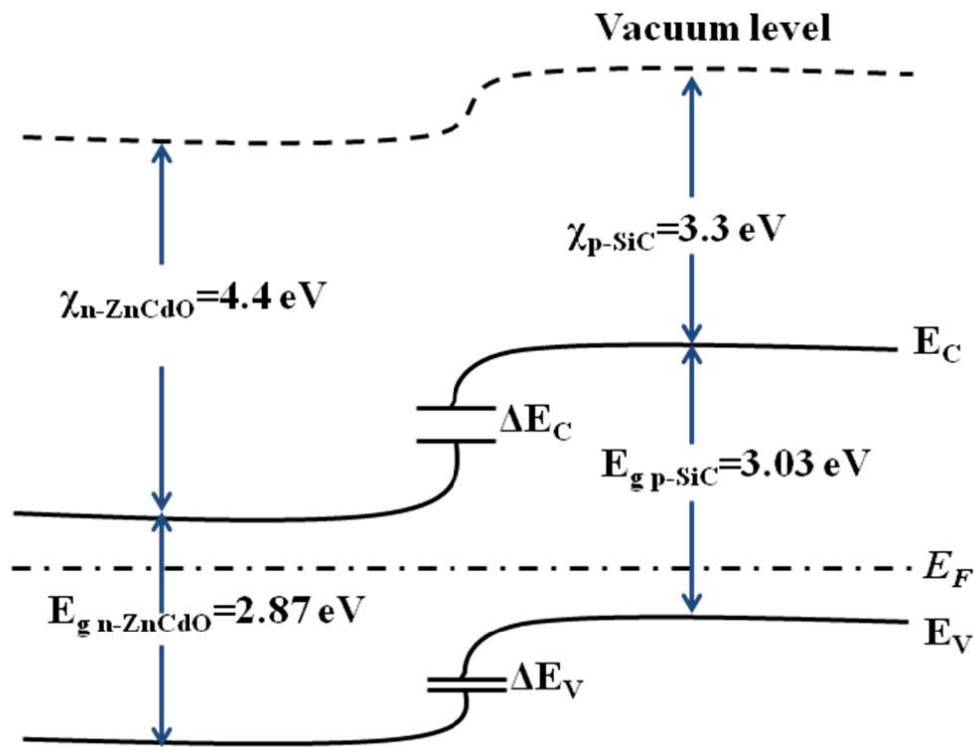

Fig.4. Band diagram (in the terms of the Anderson model [21]) of p-n heterojunction of 6H-p-SiC and n-ZnCdO.

Since the electron injection from n-ZnCdO into p-SiC has a larger energy barrier than the hole injection from p-SiC into n-ZnCdO, the light emission should mainly originate from the n-ZnCdO areas. Similar result was reported in [6] for n-ZnCdO/p-GaN heterojunction. It was noticed that the conduction band offset ΔE_C is much larger than the valence band offset ΔE_V [6]. Therefore, the radiative recombination occurs in the n-ZnCdO semiconductor layer [6]. In this context, results of PL studies of our heterostructures are very informative since they should conform to electroluminescence (EL) data.   Figure 5 shows the photoluminescence spectra of the

heterojunctions at room temperature. There can be seen a broad band located in blue-green region (380-600 nm) and a spectral band falling into the region between 600 and 720 nm. The near-band-edge emission should be attributed to radiative recombination processes in ZnCdO caused by alloy-fluctuation-induced exciton localization. The deep-level visible emission is caused by the presence of various point defects such as oxygen vacancies and interstitial Zn ions in the ZnCdO lattice [24, 25]. The spectral region of 380-600 nm for the n-ZnCdO grown on p-SiC can be reconstructed by three Gaussian curves (Insert of Fig. 5) with peaks at around 386 nm (3.21 eV), 431 nm (2.87 eV), and 487 nm (2.54 eV).
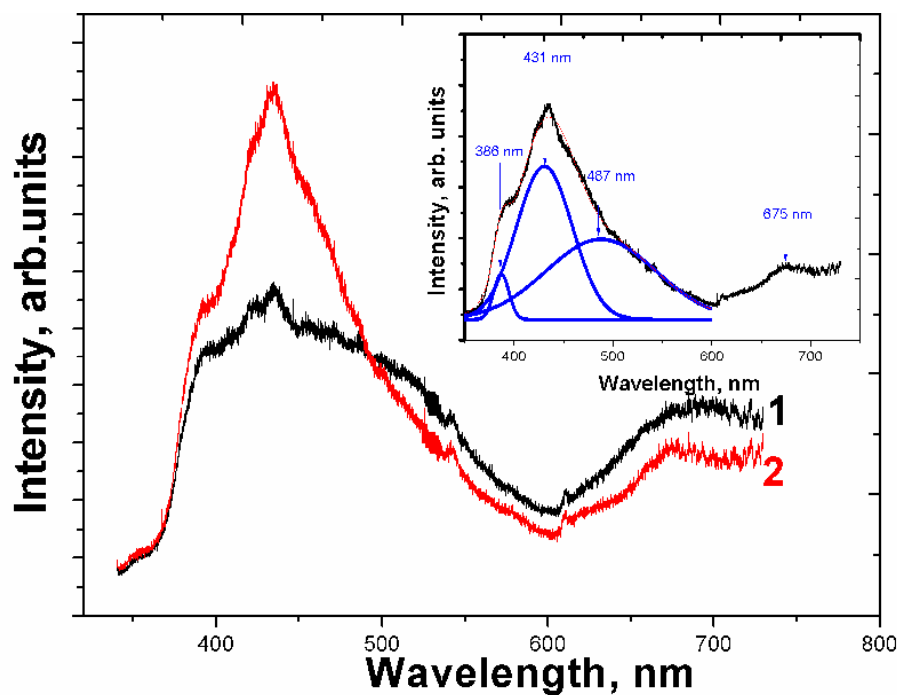

Fig.5. Room temperature photoluminescence spectra of the n-ZnCdO/p-SiC heterojunctions: p (curve 1) and p$^+$(curve 2)-substrates.

The asymmetric nature of the luminescence band may be associated with the overlapping several emission lines responsible for the exciton localization in cadmium-rich regions of the film (or recombination processes related to defect subsystem of ZnO). In other words, the large spectrum width may be mainly due to alloy composition fluctuation in the ZnCdO layer. In this sense, the luminescence of these samples can be explained by the effect of exciton localization induced by

compositional fluctuation of Cd, where the pathways of nonradiative recombination centers may be hindered once excitons are captured at potential minima. Therefore, such features of PL emission give an evidence of a possible existence of the Cd-rich regions which would correspond to higher cadmium content. It can be explained by the nonuniform distribution of cadmium. We have studied a map of the lateral distribution of the cadmium ions by means of the EDX analysis in the SEM. An SEM image of the film surface as well as the corresponding map sum EDX spectrum is demonstrated in Fig. 6. We observed a rather uniform distribution of the Cd elements over the surface. And only slight correlation may be observed for morphology and grain boundaries with Cd signal intensity (green points on the SEM image shown in Fig. 6). The later may be responsible for the specific behavior of the PL spectra of the ZnCdO ternary alloys. Actually, the obtained visible photoluminescence of ZnCdO is very interesting for a design of white LEDs. It is due to the fact that the combination of different visible emission bands can be regarded as white light.
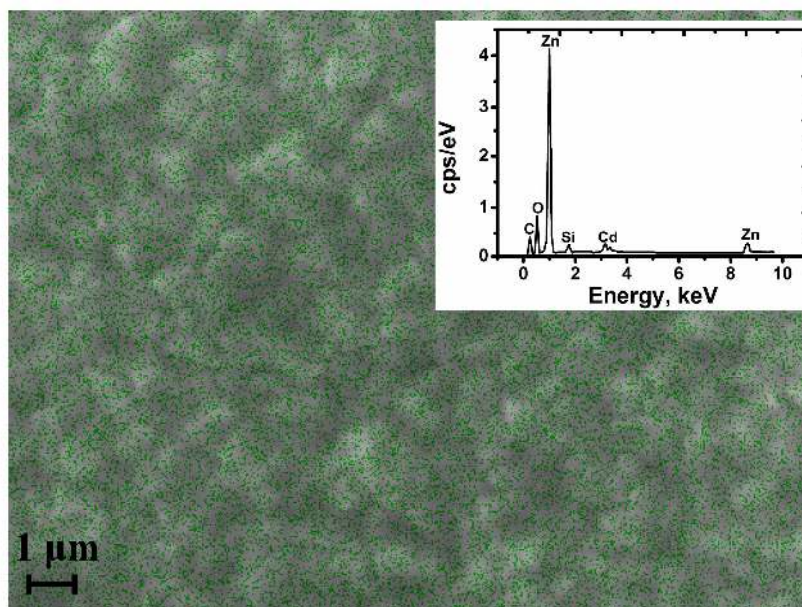

Fig. 6 Map of the lateral cadmium distribution for the film ZnCdO grown on the 6H-SiC substrates. Inset is corresponding EDX spectrum.

Fig. 7 demonstrates current–voltage (I-V) characteristics of the n-ZnCdO on p and p⁺-SiC substrates at room temperature, which have different turn-on voltages of 4.4 and 3 V, respectively. These high turn-on voltages may be related to the presence of a poor ohmic contact ~~at the interface~~ between 6H-SiC and the electrodes, which is a challenging issue. The I-V curves show a clear rectifying behavior. Such type of rectification behavior is best described by the thermionic emission theory [26]. Recently, there were reported turn-on voltages of 3.9 V for n-ZnCdO/p-GaN heterostructure [6], 6 V for ZnCdO MQW LEDs [15], 2.5 V for The Zn1-xCdxO-NRs/p-GaN LED [13] and 5 V for p-n heterojunction based LED structure (n-Zn1-xCdxO/p-GaN:Mg)/sapphire/Cu) [14]. Therefore, n-ZnCdO/p-SiC hetero-structures possess similar performances (turn-on voltage ~3-4.4 V) compared to those reported in the literature. Some difference in the values of the threshold voltage between different heterostructures is associated with (i) unique type and area of the ohmic contacts, (ii) different cadmium content in ZnCdO active layer and (iii) different concentration of the interface defects.
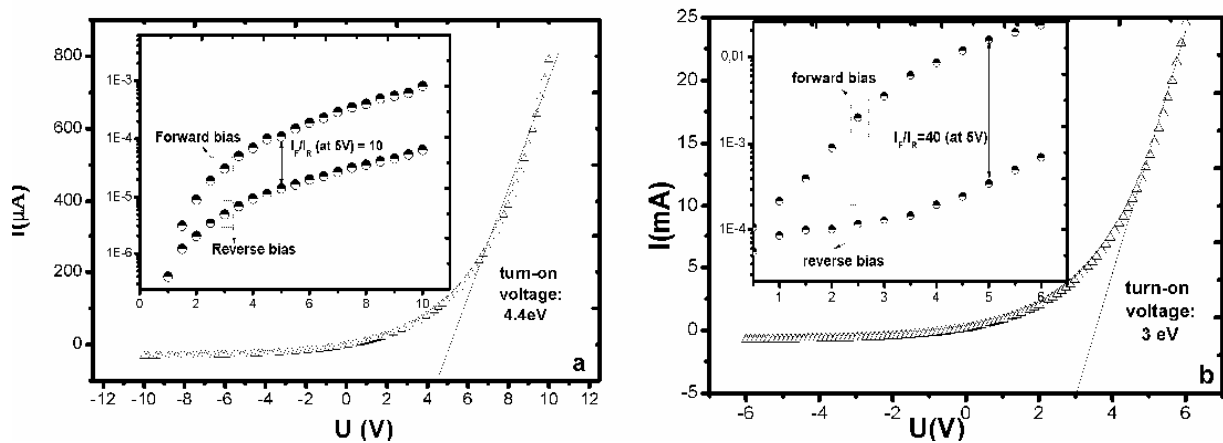

Fig.7. I-V characteristics of Al/n-Zn$_{0.9}$Cd$_{0.1}$O/p-SiC/Ni/Cr/Al (a) and (b) Al/n-Zn$_{0.9}$Cd$_{0.1}$O/p⁺-SiC/Ti/Al heterojunction diodes at room temperature. The inset shows a semi-log plot of the I−V characteristics of n-ZnCdO/p and p⁺-SiC heterojunction diodes. The values show the forward current (I$_F$) and reverse current (I$_R$) ratios at ±5 V.

The ideality factor was estimated from the I–V plot using the diode equation [26] and was obtained for both diodes to be >4. The large magnitudes of the ideality factor suggest that the mechanism of transport is no longer prevailed by the thermionic emission. Non-ideal behavior is often related to defect states in the band gap of the semiconductor. It provides other mechanisms of current transport such as structural defects, generation - recombination in the space charge region, barrier tunneling, or surface contamination [27, 28]. It is expected for heterojunction diodes which inescapably have more defect states at the interface due to the lattice and valence mismatch, and alloy fluctuations in ZnCdO.

The inset in Fig. 7a shows a plot of log(I) vs. voltage [29]; when the reverse bias reaches 5 V, n-ZnCdO/p-SiC has a small reverse leakage current of about 10^{-5} A. Moreover, the ratio of the forward current to the reverse current (I_F/I_R) at ±5 V is low, being approximately 10. Figure 7(b) shows the I-V characteristics of the ZnCdO film grown on p^+-SiC substrate; it has turn-on voltages of 3 V. The value of I_F/I_R at 5 V for this heterostructure is about 40. For a reverse bias of 5 V, the leakage current of the n-ZnCdO/p^+-SiC is 10^{-4} A. Among the two heterostructures, the one on the p^+-SiC substrate has a higher leakage current. These results indicate that heavy doping of the p^+-SiC makes a tunneling current more probable [30]. Nevertheless, the heterojunction diode fabricated from ZnCdO grown on p^+-SiC exhibited more stable rectification characteristics and higher value of I_F /I_R. The diode series resistance determined as $Rs = dV/dI$ [31] is depicted in Figure 8. Below the turn-on voltage, Rs lowers with increasing the forward bias. Then it keeps a changeless value above the turn-on voltage.
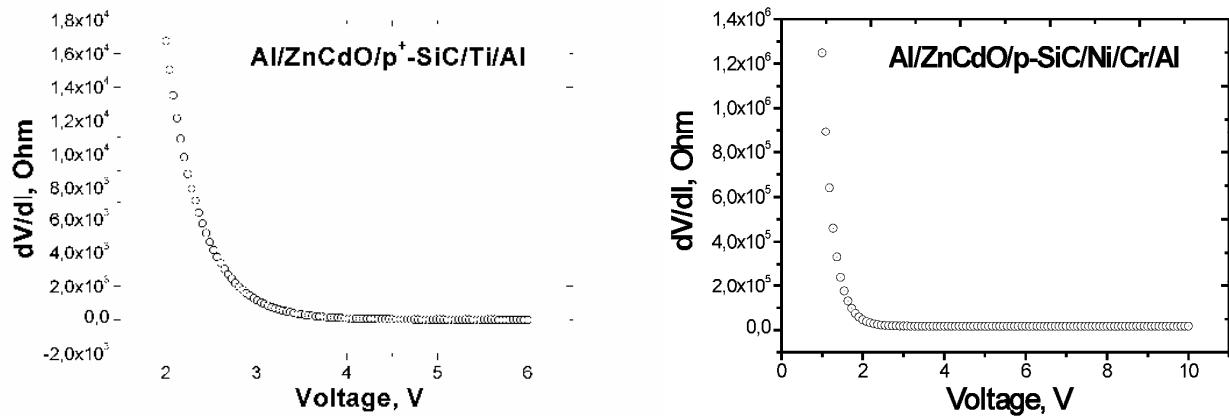
Fig. 8. Diode resistance dV/dI as a function of voltage for studied heterostructures

At the forward bias the conduction band barrier will be lowered and will increase the electron stream from the n-ZnCdO to the p-SiC and holes from the p-SiC to the n-ZnCdO. The tunneling recombination would give rise to the forward bias current flow. When the forward bias is high enough, the barrier is insignificant; therefore the diode resistance gets invariable, which is associated with the series resistance of bulk material [32]. The sluggish increase of the forward current at the low bias could be stimulated by the distribution of the voltage of the nonideal contact between ZnCdO film and Al electrode. When $I/(dI/dV)$ is plotted against I, as shown in Fig. 9(a) for ZnCdO/p$^+$-SiC and in Fig. 9(b) for ZnCdO/p-SiC, the slope is R_S [31]. Diode series resistances in the range of 166 Ω to 3.865 kΩ depend on acceptor concentration. Taking into account the value of the turn-on voltages for both heterostructures we have concluded that there is a possibility to reduce the values of the observed turn-on voltages by decreasing series resistance. Series resistance can be reduced by improving the quality of metal contacts, and by increasing the doping levels of SiC layers.
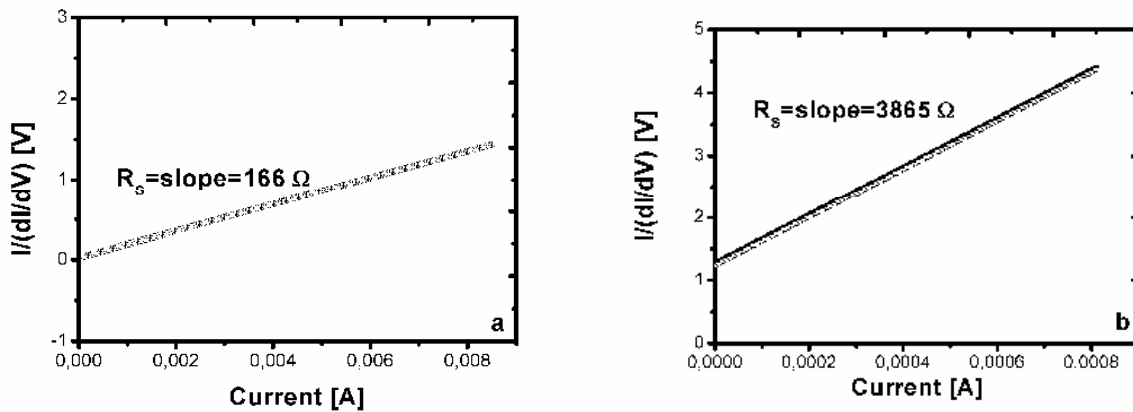
Fig.9. I/(dI/dV) plots of n-ZnCdO/p+(a) and p (b)-SiC heterojunction diodes, together with the

series resistances.

Alloy fluctuations are expected to affect the electrical properties severely (and possible electroluminescence features) of the heterostructures. Since the spatial cadmium distribution in the volume of the film is nonuniform, then small and large alloy compositional fluctuations may take place simultaneously (as shown in the Fig. 10). At the low forward currents the carriers may be easily captured to localized energy states generated by alloy compositional fluctuations and radiatively recombine before they are trapped by non-radiative recombination centers formed by a lot of dislocations and structural defects. When the forward current is increased, some injected carriers can overflow [32] from the shallow localized energy states due to lowering the potential barriers (or small compositional fluctuation in ZnCdO) and reach the non-radiative recombination centers [32, 33]. In this case, a decrease in efficiency of the n-ZnCdO/p-SiC heterojunction will be expected. On the other hands, if the degree of compositional fluctuations is high enough, the efficiency of the radiative recombination may reach a high value due to a large number of deep localized energy states formed by large alloy compositional fluctuation. In this case, the non-radiative optical transitions may be blocked due to strong exciton localization, i.e. the injected carriers into ZnCdO layer are still confined even at high current operation. Nevertheless, further improvement of the performance of the ZnCdO-based devices requires clear understanding of the correlation mechanisms in terms of the triad "degree of alloy fluctuation - probability of the radiative recombination processes – defect concentration".
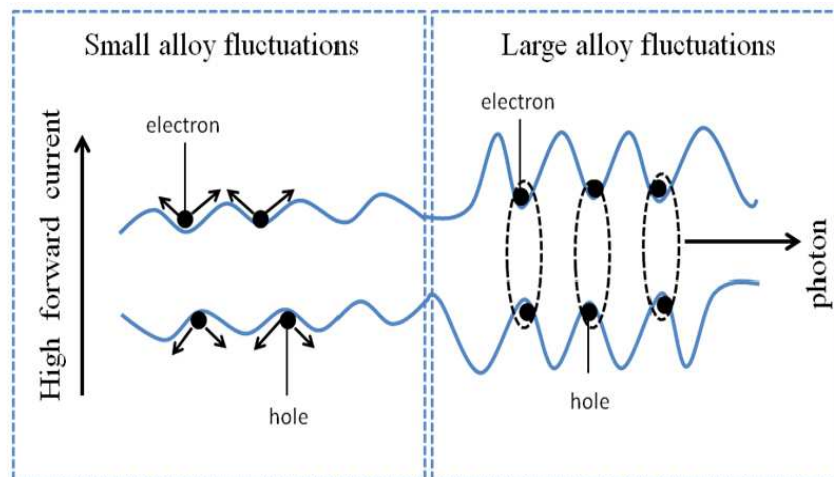
Fig. 10. A schematic model of localized energy states formed by alloy composition fluctuations. This model was first proposed by S. Nakamura [33]

Conclusions

We have fabricated n-ZnCdO/p-SiC heterostructures at low temperatures by using direct current magnetron sputtering technique. Due to the realization of the Cd-to-Zn substitution mechanisms, the energy barrier for holes was found to be lowered and intensive hole injection from p-SiC to n-ZnCdO occurred. This resulted in the radiative recombination occurring mainly in the n-type material. The heterostructures exhibited reasonable rectification behavior and diode characteristics, having turn-on voltages in the range from 3 to 4.4 V and series resistance from 166 to 3865 Ω depending on the acceptor concentration in SiC layer. Obtained heterostructures possess similar performances (turn-on voltage ~3-4.4 V) compared to those reported in the literature. The visible luminescence demonstrated from the ternary alloys represents a significant application interest that should support efforts to develop ZnCdO-based devices such as white light emitting diodes.

Acknowledgements

References

[1] G. V. Lashkarev, V. A. Karpyna, V. I. Lazorenko, A. I. Ievtushenko, I. I. Shtepliuk and V. D. Khranovskyy, Properties of zinc oxide at low and moderate temperatures, Low Temp. Phys. 37 (2011) 226-234.

[2] V. Khranovskyy, I. Tsiaoussis, G. R. Yazdi, L. Hultman and R. Yakimova, Heteroepitaxial ZnO nanohexagons on p-type SiC, J. Cryst. Growth 312 (2010) 327 – 332.

[3] Y.T. Shih, M.K. Wu, M.J. Chen, Y.C. Cheng, J.R. Yang, M. Shiojiri, ZnO-based heterojunction light-emitting diodes on p-SiC(4H) grown by atomic layer deposition, Appl. Phys. B 98 (2010) 767–772.

[4] Y.I. Alivov, D. Johnstone, Ü. Özgür, V. Avrutin, Q. Fan, S.S. Akarca-Biyikli, H. Morkoç, Electrical and Optical Properties of n-ZnO/p-SiC Heterojunctions, Jpn. J. Appl. Phys. 44 (2005) 7281-7284.

[5] A. El-Shaer, A. Bakin, E. Schlenker A.C. Mofor, G. Wagner, S.A. Reshanov, A. Waag, Fabrication and characterization of n-ZnO on p-SiC heterojunction diodes on 4H-SiC substrates, Superlattices Microstruct. 42 (2007) 387–391.

[6] F. Fang, D. Zhao, X. Fang, J. Li, Z. Wei, S. Wang, Jilong Wu, D. Shen, X. Wang, Tunable electroluminescence from n-ZnCdO/p-GaN heterojunction, J. Phys. Chem. Solids 73 (2012) 217–220.

[7] X. Ma, P. Chen, R. Zhang, D. Yang, Optical properties of sputtered hexagonal CdZnO films with band gap energies from 1.8 to 3.3 eV, J. Alloys Compd. 509 (2011) 6599–6602.

[8]G.-R. Li, W.-X. Zhao, Q. Bu, Y.-X. Tong, A novel electrochemical deposition route for the preparation of Zn1-xCdxO nanorods with controllable optical properties, Electrochem. Commun.11 (2009) 282–285.

[9] A. Fouzri, V. Sallet, M. Oumezzine, A comparative structure and morphology study of Zn(1-x)CdxO solid solution grown on ZnO and different sapphire orientations, J. Cryst. Growth 331 (201) 18–24.

[10] I. Shtepliuk, G. Lashkarev, V. Khomyak, O.Lytvyn, P. Marianchuk, I. Timofeeva, A. Ievtushenko, V. Lazorenko, Features of the influence of the deposition power and gas ratio Ar/O$_2$ on the microstructure and optical properties of the Zn$_{0.9}$Cd$_{0.1}$O films, Thin Solid films, 520 (2012) 4772–4777.

[11] I. Shtepliuk, G. Lashkarev, V. Khomyak, P. Marianchuk, P. Koreniuk, D. Myroniuk, V. Lazorenko, I. Timofeeva, Effects of Ar/O$_2$ gas ratio on the properties of the Zn$_{0.9}$Cd$_{0.1}$O films prepared by DC reactive magnetron sputtering, Acta Phys. Pol. A 120 (2012) A61-A65.

[12] W. Lim, D. P. Norton, S. J. Pearton, X. J. Wang, W. M. Chen, A. Buyanova, A. Osinsky, J. W. Dong, B. Hertog, A. V. Thompson, W. V. Schoenfeld, Y. L. Wang and F. Ren, Migration and luminescence enhancement effects of deuterium in ZnO/ZnCdO quantum wells, Appl. Phys. Lett. 92 (2008) 032103-3.

[13] Th. Pauporte, O. Lupan, and B. Viana, Tunable electroluminescence from low-threshold voltage LED structure based on electrodeposited Zn1-xCdxO-nanorods/p-GaN heterojunction, Phys. Status Solidi A 209 (2012) 359-363.

[14] O. Lupan, Th. Pauport, T. Le Bahers, I. Ciofini, and B. Viana, High Aspect Ratio Ternary Zn1-xCdxONanowires by Electrodeposition for Light-Emitting Diode Applications, J. Phys. Chem. C, 115 (2011)14548-14558.

[15] K. Yamamoto, A. Nakamura, J. Temmyo, E. Muñoz and A. Hierro Green Electroluminescence From ZnCdO Multiple Quantum-Well Light-Emitting Diodes Grown by Remote-Plasma-Enhanced Metal–Organic Chemical Vapor Deposition, IEEE Photon. Technol. Lett., 23 (2011) 1052-1054.

[16] J.J. Brown and F.A. Hummel, Phase Equilibria and Manganese-Activated Luminescence in the Systems CdO-P$_2$O$_5$ and Zn$_2$P$_2$O$_7$-Cd$_2$P$_2$O$_7$; Summary for the System ZnO-CdO-P$_2$O$_5$, J. Electrochem. Soc. 111/ 9 (1964) 1052-1057.

[17] F. Bertram, S. Giemsch, D. Forster, J. Christen, R. Kling , C. Kirchner, A. Waag, Direct imaging of phase separation in ZnCdO layers, Appl. Phys. Lett. 88 (2006) 061915-3.

[18] V. Venkatachalapathy, A. Galeckas, M. Trunk, T. Zhang, A. Azarov, and A.Yu. Kuznetsov, Understanding phase separation in ZnCdO by a combination of structural and optical analysis, Phys. Rev. B 83 (2011) 125315-11.

[19] A.I. Ievtushenko, G.V. Lashkarev, V.I. Lazorenko, V.A.Karpyna, M.G. Dusheyko, V.M. Tkach, L.A. Kosyachenko, V.M. Sklyarchuk, O.F. Sklyarchuk, K.A. Avramenko, V.V. Strelchuk, Zs.J. Horvath, Effect of nitrogen doping on photoresponsivity of ZnO films, Phys. Stat. Sol. (a), 207 (2010) 1746–1750.

[20] P. Sagar, P.K. Shishodia, R.M. Mehra, H. Okada, A. Wakahara, A. Yoshida, Photoluminescence and absorption in sol–gel-derived ZnO films, J. Lumin. 126 (2007) 800-806.

[21] A.G. Milnes and D.L. Feucht, Heterojunctions and Metal-Semiconductor Junctions, Academic, New York, 1972.

[22] R. Ferro, J.A.Rodrı´guez, Influence of F-doping on the transmittance and electron affinity of CdO thin films suitable for solar cells technology, Sol. Energy Mater. Sol. Cells 64 (2000) 363-370.

[23] V. Khranovskyy and Rositza Yakimova, Heteroepitaxy of ZnO on SiC as a route toward nanoscale p-n junction, in: Z. C. Feng (Eds.), Handbook of ZnO and related materials, Taylor and Francis/CRC Press, Florida, USA, 2012.

[24] D. W. Ma, Z. Z. Ye, and L. L. Chen, Dependence of structural and optical properties of Zn1-xCdxO films on the Cd composition, Phys. Status Solidi A 201 (2004) 2929-2933.

[25] W. F. Yang,R. Chen,B. Liu,G. G. Gurzadyan, L. M. Wong, S. J. Wang, and H. D. Sun, Surface-plasmon enhancement of band gap emission from ZnCdO thin films by gold particles, Appl. Phys. Lett. 97 (2010) 061104-3.

[26] S. M. Sze, Physics of Semiconductor Devices (Wiley, New York, 1981)

[27] M.W. Allen and S. M. Durbin, Influence of oxygen vacancies on Schottky contacts to ZnO, Appl. Phys. Lett. 92 (2008) 122110-122110-3.

[28] D.T. Quan and H. Hbib, High barrier height Au/n-type InP Schottky contacts with a $PO_xN_yH_z$ interfacial layer, Solid-State Electron. 36 (1993) 339–344.

[29] J. H. Lee, J. Y. Lee, J. J. Kim, H. S. Kim, N. W. Jang, W. J. Lee, C. R. Cho, Dependence of the diode characteristics of n-ZnO/p-Si (111) on the Si substrate doping, J. Korean Chem. Soc. 56 (2010) 429-433.

[30] X. Li, B. Zhang, X. Dong, Y. Zhang, X. Xia, W. Zhao and G. Du, Room temperature electroluminescence from ZnO/Si heterojunction devices grown by metal–organic chemical vapor deposition, J. Lumin. 129 (2009) 86-89.

[31] X. D. Chen, C. C. Ling, S. Fung, C. D. Beling, Y. F. Mei, K. Y. Ricky, G. G.Siu, P. K. Chu, Current transport studies of ZnO/*p*-Si heterostructures grown by plasma immersion ion implantation and deposition, Appl. Phys. Lett. 88 (2006) 132104-132104-3.

[32] N. Bano, I. Hussain, O. Nur, M. Willander, P. Klason, Study of radiative defects using current-voltage characteristics in ZnO rods catalytically grown on 4H-p-SiC, Journal of Nanomaterials 2010 (2010) 1-5.

[33] S. Nakamura, Current status and future prospects of InGaN-based laser diodes, JSAP Int. 1 (2000) 5-17.

[34]. S. Nakamura, The roles of structural imperfections in InGaN/GaN/AlGaN-based laser diodes grown on GaN substrates with a fundamental transverse mode, Science 281, 956–961 (1998).